Study of Intermicellar Interactions and Micellar Sizes in Ionic Micelle Solutions by Comparing Collective Diffusion and Self-Diffusion Coefficients

Luciano Galantini,*,† Salvatore Marco Giampaolo,† Luisa Mannina,‡,§ Nicolae Viorel Pavel,† and Stéphane Viel‡,§

Dipartimento di Chimica, Università di Roma "La Sapienza", P.le A. Moro 5, 00185 Roma, Italy, Istituto di Metodologie Chimiche, CNR, C.P. 10, Via Salaria km. 29.300, I-00016 Monterotondo Stazione, Italy, and Facoltà di Agraria, Dipartimento S.T.A.A.M., Università del Molise, Via De Sanctis, I-86100 Campobasso, Italy

Received: November 3, 2003; In Final Form: February 12, 2004

Dynamic light scattering and pulsed gradient spin−echo NMR measurements were performed on D_2O solutions of sodium glycocholate (NaGC). The micelle self-diffusion and collective diffusion coefficients were measured for 0.08 M NaGC solutions at different added NaCl molarities (0.1−0.8 M). Moreover, a study as a function of NaGC concentration at 0.1 M NaCl was performed. Both the surfactant and the NaCl concentration dependencies of the diffusion coefficients were interpreted on the basis of the DLVO theory of colloidal stability. The experimental data were analyzed by considering both the effect of micellar growth and interaction potential variation. The micelle ionization degree α was supposed to be constant over the range of 0.03−0.10 M NaGC and 0.1 M NaCl, whereas no restriction was imposed on its NaCl concentration dependence. The NaGC critical micelle concentrations at all of the studied NaCl molarities were inferred from surface tension measurements on NaGC H_2O solutions. The best-fit micellar hydrodynamic radii and aggregation numbers point out that very slight micellar growth is induced by increasing the added electrolyte and/or the surfactant concentration. Moreover, the α value slightly decreases by increasing the NaCl molarity. An interpretation model of monodisperse spherical particles with a hard-core interaction shell of suitable thickness was also used to interpret the data at low ionic strength (from 0.1 to 0.4 M NaCl). Satisfactory agreement between the two interpretation models is obtained.

I. Introduction

The determination of both collective and self-diffusion coefficients of colloidal particles represents one of the most useful methods of studying colloidal systems. Both of these coefficients coincide at the limit of infinite dilution and can be related to the particle hydrodynamic radius by means of the Stokes−Einstein equation. However, it is experimentally observed that the particle concentration affects the diffusion coefficients. Normally, particle interactions are invoked to justify this phenomenon, hence diffusion coefficients of colloidal dispersions are studied by extrapolating the experimental data to infinite dilution. In this way, information on the particle hydrodynamic radius and particle interactions are inferred from the intercept and the slope of the extrapolated curve.

However, this extrapolation is impossible when self-assembling systems are studied because, very often, the assembled aggregates change their size and shape by varying the particle volume fraction. Therefore, particle growth affects the diffusion coefficient concentration dependence. In particular, ionic micelle solutions follow this kind of behavior because the ionic micelles grow by increasing either the amphiphile concentration or the ionic strength. Likewise, several experimental data show that ionic micelle diffusivity depends on the surfactant and added electrolyte concentration.[1−17] Of course, a combination of the particle interaction effect and micellar size variation must be considered to explain the experimental trends.

According to the standard DLVO theory of colloidal stability,[18] the direct interaction potential between two ionic micelles is generally expressed as the sum of three independent parts: (i) a hard-body repulsion representing the excluded volume effect of the micelles, (ii) an electric double-layer repulsion between two micelles surrounded by their own ionic atmosphere, and (iii) a long-range van der Waals attraction. Generally, the repulsive electrostatic potential prevails on the attractive one in ionic micelle solutions at low ionic strength. However, by increasing the ionic strength, the electrostatic interaction becomes more and more screened, and beyond a critical point, the attractive potential prevails. At low added electrolyte concentration, particle correlation appears to be the most important factor influencing the micelle diffusion because of the repulsive electrostatic interactions. Models based exclusively on intermicellar interactions have been proposed to explain the diffusivity data under these conditions, thus allowing the definition of the DLVO interaction potential.[3,9] However, no exhaustive methods have been proposed to interpret the data at high ionic strength, where the attractive potential dominates and micellar growth is expected to sensitively affect the experimental data.

In previous papers, we proposed a comparative analysis of collective and self-diffusion coefficients to extract information on micelle geometry and the intermicellar interaction potential without performing any concentration-dependence study.[13,14] Ionic micelle solutions at low ionic strengths were investigated. Therefore, by assuming an essentially repulsive interaction

* Corresponding author. E-mail: l.galantini@caspur.it. Tel: (+39)-6-49913687. Fax: (+39)-6-490631.
† Università di Roma.
‡ CNR.
§ Università del Molise.

10.1021/jp037328+ CCC: $27.50
Published on Web 03/20/2004

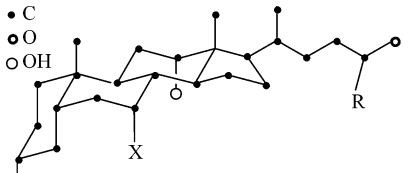

TDC: X=H R=NH-CH_2-CH_2-SO_3^-
GDC: X=H R=NH-CH_2-CO_2^-
TC: X=OH R=NH-CH_2-CH_2-SO_3^-
GC: X=OH R=NH-CH_2-CO_2^-

Figure 1. Formulas of some bile salt anions. The symbols GDC, TDC, GC, and TC refer to glycodeoxycholate, taurodeoxycholate, glycocholate, and taurocholate anions, respectively.

potential, an interpretation model of monodisperse spherical particles with a hard-core interaction shell of suitable thickness was used to represent the micelle dispersion ideally.[19] In this work, the above-mentioned comparative analysis is performed by using the whole DLVO interaction potential. This procedure does not impose any restriction on the interaction potential character, thus also allowing the discussion of systems where the attractive component dominates. In this way, a method to define the micellar size as well as the particle interaction potential from diffusivity measurements, over the whole ionic strength range of existence of a micellar solution, is provided.

Previously[13,14] we investigated the micellar solutions of some bile salts (Figure 1), which are extremely important biological surfactants mainly because of their ability to solubilize and to carry a wide variety of molecules in aqueous physiological solutions. D_2O solutions of sodium taurocholate (NaTC) and taurodeoxycholate (NaTDC) with different concentrations of added NaCl were studied. Dynamic light scattering (DLS) and pulsed gradient spin−echo NMR (PGSE-NMR) measurements were used to determine the micelle collective and self-diffusion coefficients. The micellar growth induced by increasing the bile salt and the added electrolyte concentrations was studied by means of diffusivity data. In this work, sodium glycocholate (NaGC) D_2O solutions at different surfactant and NaCl concentrations are investigated.

In section II, the material and the experimental data acquisition are described. In the theoretical section (section III), we present a description of the diffusion coefficients, obtained by DLS and PGSE-NMR, on the basis of the DLVO interaction potential and the hard-core interaction model used in refs 13 and 14. In section IV, the experimental results are reported and discussed in the framework of the theoretical model described in section III. Finally, section V summarizes the conclusions.

II. Experimental Section

Materials. D_2O (100%, Aldrich), NaCl (Merck, suprapur), and hexametildisilane (Me_6Si_2) (98%, Aldrich) were used. NaGC (Sigma) was crystallized from a mixture of water and acetone.

Surface Tension Mesurements. The surface tension γ was measured by the ring detachment method with a computerized Lauda apparatus. During the measurements, the samples were maintained at 27.0 ± 0.1 °C by a suitable thermostatic apparatus.

DLS Measurements. In the DLS experiment, the temporal fluctuations of the scattered intensity, which are due to the particle Brownian motion, have been analyzed by estimating the normalized temporal autocorrelation function of the scattered intensity

$$g_2(q, \tau) = \frac{\langle I(q, 0)\, I(q, \tau)\rangle}{\langle I(q)\rangle^2} \qquad (2.1)$$

where $I(q, \tau)$ is the scattered intensity at scattering vector q and at time τ. By assuming a Gaussian distribution of the intensity profile, the normalized field autocorrelation function $g_1(q, \tau)$ has been derived from $g_2(q, \tau)$ through the Siegert relation:[20,21]

$$g_2(q, \tau) = 1 + B|g_1(q, \tau)|^2$$

Therefore, $g_1(q, \tau)$ has been analyzed through the cumulant expansion, and the so-called apparent diffusion coefficient D_{app} has been obtained from the first cumulant by the relation

$$D_{app} = -\frac{1}{q^2}\frac{\mathrm{d} \ln g_1(q, \tau)}{\mathrm{d}\tau}\Big|_{\tau=0}$$

A Brookhaven instrument consisting of a BI-2030AT digital correlator with 136 channels and a BI-200SM goniometer was used. The light source was a Uniphase solid-state laser system model 4601 operating at 532 nm. Dust was eliminated by means of a Brookhaven ultrafiltration unit (BIUU1) for flow-through cells, the volume of the flow cell being about 1.0 cm^3. Nuclepore filters with a pore size of 0.1 μm were used. The samples were placed in the cell for at least 30 min prior to the measurement to allow for thermal equilibration. Their temperature was kept constant within 0.5 °C by a circulating water bath. The time-dependent light-scattering correlation function was analyzed only at the 90° scattering angle. Apparent diffusion coefficients did not depend on the exchanged wave vector in the range 30−150° under our experimental conditions.

PGSE-NMR Measurements. Stejskal and Tanner have demonstrated that molecular self-diffusion can be studied by NMR by means of pulsed gradients of the magnetic field.[22] The principles and applications of the so-called PGSE-NMR technique have been thoroughly reviewed.[23−26]

Basically, in the case of the stimulated echo sequence, the NMR signal amplitude I_N of a nucleus observed at the echo is given by[27]

$$I_N = I_{NO} \exp(-D_s(\gamma g \delta)^2(\Delta - \epsilon(\delta)))$$

where I_{NO} is the resonance amplitude at zero gradient strength, γ is the magnetogyric ratio of the observed nucleus, and g, δ, and Δ are the strength, the duration, and the separation of the gradient pulses, respectively. The term $\epsilon(\delta)$ is a correction factor that depends both on δ and on the pulse sequence used, and D_s is the nucleus long-time self-diffusion coefficient. In practice, to obtain D_s, the integrated signal intensities are plotted as a function of the square of the gradient strength, and the resulting decay curve is fit (simplex algorithm) to the equation reported above. In this case, all data are well described by a single exponential.

^{1}H diffusion experiments were performed at 300 K on a Bruker AVANCE AQS600 NMR spectrometer operating at 600.13 MHz for the proton Larmor frequency and equipped with a Bruker 5-mm multinuclear inverse probe head capable of producing linear gradients with a strength of 55 G cm^{-1}. The stimulated-echo sequence incorporating bipolar gradient pulses and a longitudinal eddy current delay (BPP-LED) was used.[28] The gradient strength was logarithmically incremented in 16 steps from 2% up to 95% of the maximum gradient strength. Diffusion times and gradient pulse durations were optimized for each experiment to achieve a 95% decrease in the resonance intensity at the largest gradient amplitude; typically, diffusion times between 420 and 800 ms and bipolar sine gradient pulses

of 1.4 ms were employed. The longitudinal eddy current delay was held constant at 25 ms whereas the gradient pulse recovery time was set to 0.1 ms.

III. Data Interpretation

In the hydrodynamic limit, the characteristic probing length of the scattering experiment ($2\pi/q$) is much larger than the most probable particle distance, and $g_1(q, \tau)$ describes the spatial fluctuations of particle concentrations.[29] In the simplest case of monodisperse particles, $g_1(q, \tau)$ decays as a single exponential, and D_{app} is equal to the collective diffusion coefficient. Moreover, because of particle interaction, D_{app} is concentration-dependent, and to first order, we have

$$D_{app} = D_o(1 + \lambda_C\phi) \tag{3.1}$$

where ϕ is the particles volume fraction and D_o represents the diffusion coefficient at infinite dilution given by

$$D_o = \frac{kT}{6\pi\eta a} \tag{3.2}$$

with k, T, a, and η representing the Boltzmann constant, the absolute temperature, the hydrodynamic radius of the diffusing particles, and the medium viscosity, respectively.

Likewise, at the limit of infinite dilution of suspended particles, the long-time self-diffusion coefficient obtained by PGSE-NMR is equal to the single-particle diffusion coefficient D_o, and because of particle interaction, we write

$$D_s = D_o[1 + (\lambda_A + \alpha_S)\phi] \tag{3.3}$$

where the term λ_A accounts for the interaction effect on the self-diffusion coefficient at short time and α_S represents an additional term that must be considered when the long-time self-diffusion is treated.[19,30]

In micelle solutions, the aggregate polydispersity can complicate the diffusion coefficient analysis. In fact, D_s and D_{app} represent two different averages of the diffusion coefficient distribution in polydisperse systems of noninteracting particles.[13,31] Moreover, for polydisperse systems, the influence of particle interactions on D_{app} and D_s remains an unresolved theoretical problem. As usually occurs in the study of micellar solutions, we suppose that surfactant molecules in monomeric and micellar form are present in the investigated samples. In particular, in a micellar solution with a total amphiphile concentration c, it is assumed that a monomeric amphiphile at a critical micelle concentration cmc is in equilibrium with a micellar amphiphile at the concentration c-cmc. As a further assumption, the micelles are supposed to be monodisperse.

The scattered intensity $I(q, \tau)$ in eq 2.1 is generally dominated by the micelle contribution; therefore, D_{app} can be considered to be strictly related to the micelle diffusivity. On the contrary, the monomers contribute substantially to the bile salt self-diffusion coefficient measured by PGSE-NMR. For this reason, a hydrophobic marker molecule (Me_6Si_2) was used to measure the micellar self-diffusion coefficient.[32] To verify that the addition of Me_6Si_2 did not change the aggregation behavior, the bile salt self-diffusion coefficients were measured before and after the addiction of the marker. Under all of these conditions, the measured D_{app} and micelle D_s can be treated with eqs 3.1 and 3.3 if ϕ and D_o are supposed to be the micelle volume fraction and the free-diffusion coefficient, respectively.

DLVO Interpretation. The coefficients λ_C of eq 3.1 as well as λ_A and α_S of eq 3.3 depend on the direct and the hydrodynamic pair interactions and can be expressed in terms of the radial distribution function $g(r)$. For rigid spherical particles in the dilute gas approximation, we have that

$$g(r) = \exp\left[-\frac{V(r)}{kT}\right] \tag{3.4}$$

where r is the distance between the centers of two spheres and $V(r)$ is the pair interaction potential. In the case of particles with a radius a, the dimensionless particle distance $x = r/2a$ can be assumed, and the coefficient λ_A is expressed by the integral[30,33,34]

$$\lambda_A = 8\int_1^\infty g(x)[A_{11}(x) + 2B_{11}(x)]x^2\,dx \tag{3.5}$$

Moreover, it has been shown by Batchelor[35] that the coefficient α_S can be written as

$$\alpha_S = 4\int_1^\infty g(x)\left[W(x) - \frac{1}{2kT}\frac{dV(x)}{dx}G(x)\right]f(x)x^2\,dx \tag{3.6}$$

where the hydrodynamic function $W(x)$ is given by

$$W(x) = \frac{G(x) - H(x)}{x} + \frac{1}{2}\frac{dG(x)}{dx} \tag{3.7}$$

in terms of the functions $G(x)$ and $H(x)$ defined as

$$G(x) = 1 + A_{11}(x) - A_{12}(x) \tag{3.8a}$$

$$H(x) = 1 + B_{11}(x) - B_{12}(x) \tag{3.8b}$$

The terms $A_{ij}(x)$ and $B_{ij}(x)$ in eqs 3.5 and 3.8 are dimensionless hydrodynamic interaction functions whose asymptotic behavior is defined in ref 36. Numerical corrections are applied to these analytic expressions for x close to 1 according to refs 33, 37, and 38. The function $f(x)$ in eq 3.6 is a solution of the radial differential equation

$$\frac{1}{x^2}\frac{d}{dx}\left[x^2G\frac{df}{dx}\right] - \frac{1}{kT}\frac{dV}{dx}G\frac{df}{dx} - \frac{2H}{x^2}f = 4W - \frac{2}{kT}\frac{dV}{dx}G \tag{3.9}$$

which is derived from the two-spheres Smoluchowski equation. The solution $f(x)$ satisfies the boundary conditions

$$G\frac{df}{dx} = 0 \text{ at } x = 1 \qquad f \to 0 \text{ as } x \to \infty$$

However, as far as λ_C is concerned, it is known that it can be written as[9,15−17]

$$\lambda_C = \lambda_I - \lambda_f \tag{3.10}$$

where λ_I is proportional to the second virial coefficient and λ_f takes into account the volume fraction dependence of the friction coefficient. The thermodynamic parameter can be expressed as

$$\lambda_I = 8 + 24\int_1^\infty x^2[1 - g(x)]\,dx \tag{3.11}$$

where the first term (+8) is due to hard-sphere repulsions. As far as the λ_f value is concerned, two satisfactory treatments obtained by Batchelor[37] and Felderhof[34] are available. The results can be expressed in integral form as

$$\lambda_f = \lambda_{fo} + \int_1^\infty F(x)[1 - g(x)]\,dx \tag{3.12}$$

with λ_{fo} representing the hard-sphere contribution. The differences between the two treatments are very small, and the results obtained in the experimental data interpretation roughly agree within the esd values.[39] In this paper, we report the results obtained according to the Batchelor treatment, which gives $\lambda_{fo} = 6.55$ and

$$F(x) = 11.89x + 0.706 - 1.69x^{-1} \tag{3.13}$$

According to the DLVO theory,[18] the interaction potential $V(x)$ is the sum of an electric double-layer repulsion V_{es} and an attractive van der Waals component V_a. There are two limiting cases for which V_{es} has a known analytical form, depending on the value of the Debye−Hückel reciprocal screening length κ. This length is defined as

$$\kappa = \left(\frac{N_A e^2 I\, 10^3}{kT\epsilon\epsilon_o}\right)^{1/2} \tag{3.14}$$

where ϵ is the dielectric constant of the medium, ϵ_o is the permittivity of free space, e is the electronic charge, and I is the ionic strength defined as $I = 2(\mathrm{cmc} + c_{NaCl}) + \alpha(c - \mathrm{cmc})$, with c_{NaCl} representing the NaCl molarity and α representing the micelle ionization degree. For ionic micelles with an aggregation number n, when κ is sufficiently small or more quantitatively when $\kappa a \leq 3$

$$V_{es}(x) = \frac{n^2\alpha^2 e^2}{8\pi\epsilon_o\epsilon a(1+\kappa a)^2}\frac{\exp[-2\kappa a(x-1)]}{x} \tag{3.15}$$

where α is the micelle ionization degree. But when the double layer is thin (i.e., when $\kappa a > 3$),

$$V_{es}(x) = \frac{4\pi\epsilon_o\epsilon a\psi_o^2}{2}\ln\{1+\exp[-2\kappa a(x-1)]\} \tag{3.16a}$$

where the surface potential ψ_o is related to the micelle charge $n\alpha e$ through the expression

$$\psi_o = \frac{2kT}{e}\sinh^{-1}\frac{2\pi e\kappa^{-1}n\alpha e}{16\pi^2\epsilon_o\epsilon kTa^2} \tag{3.16b}$$

As far as the attractive van der Waals contribution is concerned, the following expression derived by Hamaker[40] is available:

$$V_a = -\frac{A}{12}\left[\frac{1}{x^2-1} + \frac{1}{x^2} + 2\ln\left(\frac{x^2-1}{x^2}\right)\right] \tag{3.17}$$

where A is the Hamaker constant.

Hard-Core Interaction Model. The diffusion coefficients can be very easily interpreted whenever the electrostatic repulsion effect prevails over the attractive one. In this case, the whole interaction potential can be considered to be the sum of the hard-body component plus an effective repulsive tail. With a very crude approximation, this tail can be represented by a rigid interaction shell of suitable thickness. In this way, the particle interaction is approximated as a hard-core repulsion at a center to center particle distance of $2b$, which is always longer or equal to the hydrodynamic diameter $2a$. In this case, according to the Cichocki and Felderhof treatment[19] for stick boundary conditions we have

$$\lambda_A = 8\int_{x_1}^{\infty}[A_{11}(x) + 2B_{11}(x)]x^2\,dx \tag{3.18}$$

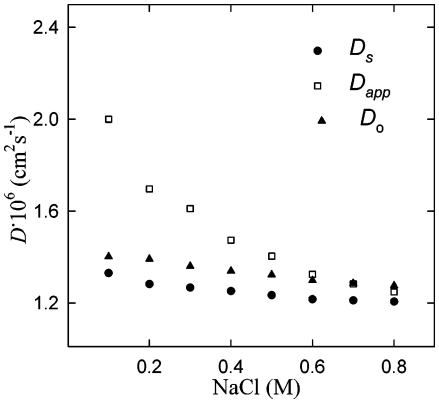

Figure 2. Experimental D_{app} and D_s and calculated D_o values obtained by the DLVO interpretation model (Table 1) for an 80 mM NaGC D_2O solution as a function of NaCl concentration at 27 °C. esd's of the experimental data are within 2%.

and

$$\alpha_S = 4\int_{x_1}^{\infty}W(x)\,f(x)x^2\,dx \tag{3.19}$$

where $x_1 = b/a$. Moreover, λ_C can be expressed as

$$\lambda_C = 8x_1^3 - 6x_1^2 + 1 + \lambda_S + \lambda_A \tag{3.20}$$

where the first three terms account for the virial correction, the Oseen contribution, and the dipole contribution, respectively, whereas the term λ_S is given by

$$\lambda_S = 8\int_{x_1}^{\infty}\left[A_{12}(x) + 2B_{12}(x) - \frac{3}{2x}\right]x^2\,dx \tag{3.21}$$

Values of λ_C and of the term $\lambda_A + \alpha_S$ as a function of x_1 can be obtained by numerically solving eqs 3.18−3.21. A polynomial approximation to these numerical values can be performed. Over the range of $1 \leq x_1 \leq 1.6$, this approximation gives rise to the following equations:

$$\lambda_C = -2.6563 + 3.5788x_1 - 7.8558x_1^2 + 8.3880x_1^3 \tag{3.22}$$

$$\lambda_A + \alpha_S = -8.9013 + 14.0894x_1 - 7.5122x_1^2 + 0.2310x_1^3 \tag{3.23}$$

The power series in these equations was interrupted at the lowest power value that gave an apparently random distribution of residuals.

IV. Results and Discussion

The micelle diffusion coefficients in NaGC 0.08 M D_2O solution as a function of NaCl concentration (0.1−0.8 M) and at 27 °C are reported in Figure 2. Trends very similar to those of the previously studied NaTC and NaTDC are observed.[13,14] In particular, at low ionic strength, where a strong electrostatic component characterizes the intermicellar interaction potential, D_{app} values much higher than D_s are obtained. However, the difference between these two values tends to decrease by increasing the NaCl concentration.

Of course, both the micellar growth and the interaction potential variation are expected to affect the experimental trends. As shown in eqs 3.1 and 3.3, an estimate of ϕ is needed to determine the particle interaction effect. These data can be calculated if a specific micellar volume per monomer v and the

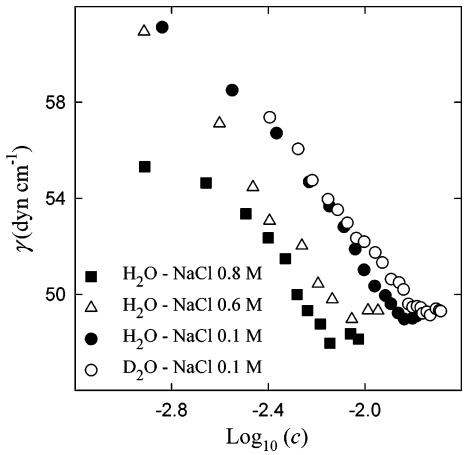

Figure 3. Surface tension γ as a function of the decimal logarithm of NaGC concentration c (mM) at different NaCl molarities and at 27 °C.

cmc are known as $\phi = (c\text{-cmc})N_A v$, where N_A is the Avogadro constant. A reasonable v value could be obtained from the NaGC molar volume V as $v = V/N_A = 608$ Å^3.[41] Actually, this value is underestimated because it does not consider the hydration water molecule contribution to the micelle volume. Recently, a v value of 900 Å^3 has been estimated for micellar aggregates of sodium glycodeoxycholate (NaGDC) on the basis of a comparative analysis of DLS and small-angle X-ray scattering (SAXS) measurements.[42] This value is in agreement with the one that can be estimated on the basis of the hydrodynamic radii and the aggregation number data reported in the literature. In view of the similarity between the glycocholate and the glycodeoxycholate anions (Figure 1), this value has been assumed to interpret the NaGC data.

The cmc values were determined by means of surface tension (γ) measurements. Some measured γ versus log(c) curves are reported in Figure 3. The results for all of the studied solutions are summarized in Table 1. Of course, samples of NaGC in D_2O should be examined for our calculations. Actually, the results obtained at 0.1 M NaCl show that, at a fixed added electrolyte concentration, similar γ curves (Figure 3) and cmc values (Table 1) characterize D_2O and H_2O solutions. For this reason, the cmc's in H_2O solutions were used to interpret the diffusivity data over the range of 0.2−0.8 M NaCl.

In this framework, as a first approach, the hard-core interaction model (HC model) described in section III has been used to interpret the diffusivity data. Therefore, assuming that ϕ is derived from the above-mentioned v value, the system of eqs 3.1, 3.3, 3.22, and 3.23 was solved to obtain x_1 and D_o. The results obtained with this interpretation are reported in Table 1. In the same table the hydrodynamic radii, estimated from the D_o values by means of eq 3.2, are listed. For each sample the viscosity of the corresponding NaCl D_2O solution has been considered (Table 1). This value was estimated by multiplying the NaCl H_2O solution viscosity for the $\eta^*_{D_2O}/\eta^*_{H_2O}$ ratio to correct for the isotopic effect (η^* being the pure solvent viscosity.)

An inspection of the reported data points out a decrease of x_1 by increasing the NaCl concentration, which testifies to a progressive screening of the intermicellar electrostatic repulsions. Obviously, among the samples of Figure 2, only those for which the repulsive interaction potential prevails on the attractive one can be described by the HC model. This condition can be considered valid whenever the solution of the above-mentioned equation system leads to $x_1 \geq 1$. For our experimental data, this is verified up to 0.4 M NaCl. Roughly speaking, this result means that van der Waals attraction dominates the tail of the DLVO interaction potential beyond this NaCl concentration.

The diffusion coefficients of micellar solution at 0.1 M NaCl and different NaGC molarities are reported in Figure 4. The corresponding D_o, a, and x_1 values estimated on the basis of the HC model are listed in Table 2. In this case, an almost constant x_1 value testifies to the interaction potential invariance.

Afterward, the diffusivity data were analyzed on the basis of the DLVO interaction potential described in section III. According to eqs 3.1−3.17, D_{app} and D_s depend on the four unknown parameter n, a, α, and A. However, if spherically or slightly anisotropically shaped micelles are treated, then a micellar volume of $4\pi a^3/3$ can be assumed, and the number of variables can be reduced by expressing the micelle aggregation number as $n = 4\pi a^3/3v$. This assumption can be reasonably accepted for the essentially globular NaGC micellar aggregate. Hence the data can be fit by assuming only a, α, and A as independent variables. First, the data of Figure 4 were treated. Because only the two values of D_{app} and D_s are available, it is impossible to fit all three parameters for each solution. However, they can be obtained by fitting the data of two or more solutions because some further relationships between α and A in different samples can be assumed. In detail, if the same monomer density characterizes the micelles under all of the investigated conditions, then A is expected to be constant for all of the samples.[43]

Moreover it is reasonable to assume that the same α can be considered for all of the samples of Figure 4 because they fall in a small range of NaGC concentration (0.03−0.1 M) and present a constant NaCl molarity.

On these bases, the data of Figure 4 were interpreted by calculating, as a first step, the a_i, a_j, A, and α values for two selected samples i and j from their experimental D_{app} and D_s. Hence, by assuming the A and α values so estimated as known parameters, the data for all of the remaining samples were fit by varying only the hydrodynamic radius a in a minimization procedure. Equation 3.15 was used to express the electrostatic potential. It is important to note that the expression for V_a makes the integrals in eqs 3.5, 3.6, 3.11 and 3.12 divergent. Therefore, a lower cutoff of $x_L > 1$ must be imposed in the calculation. The value of $x_L = 1.04$ was used, as generally assumed in the literature to describe the collective diffusion in micelle systems.

Different sample pairs were tested to start the minimization procedure; the best fit of all of the experimental data was reached by choosing the two solutions at 0.05 and 0.08 M NaGC. The calculated apparent and self-diffusion coefficients (D_{appc} and D_{sc}) are reported in Figure 4. As fitting parameters, $\alpha = 0.6(1)$ and the data listed in Table 2 were obtained. As shown in Figure 4, satisfactory agreement between calculated and experimental data is obtained.

Finally, the remaining solutions of Figure 2 were interpreted. In this case, assuming the A value obtained from the analysis of the 0.1 M NaCl solutions of Figure 4 to be a known parameter, a and α were estimated from the experimental D_{app} and D_s. Therefore, no restriction on the α values of solutions at different NaCl concentrations was imposed. Equations 3.15 and 3.16 were used to express the electrostatic potential at NaCl concentrations ≤0.3 M and >0.3 M, respectively. The calculated data are reported in Table 1.

We observed that slight changes in the cutoff length x_L (1.04 ± 0.02) do not sensitively affect the fitting parameters in Tables 1 and 2. On the contrary, the Hamaker constant is strongly dependent on these changes, thus rendering its best-fitting absolute value rather meaningless.

TABLE 1: Micellar Free-Diffusion Coefficient D_0 ($cm^2\ s^{-1}$), Hydrodynamic Radius a (Å), x_1 Value, Interaction Shell Thickness t, Ionization Degree α, Debye−Hückel Screening Length κ^{-1}(Å), and Aggregation Number n for NaGC 0.08 M D_2O Solutions, as a Function of NaCl Concentration (M), Obtained on the Basis of the HC and the DLVO Interaction Models[a]

			HC model				DLVO model				
NaCl	cmc	η	$D_o \times 10^6$	a	x_1	t	$D_o \times 10^6$	a	α	κ^{-1}	n
0.1	10(3)[b]	1.059	1.50(3)	13.8(4)	1.36(4)	4.9(6)	1.40(5)	14.7(6)	0.6(1)	8.38(9)	15(2)
0.2	9(2)	1.069	1.42(3)	14.5(3)	1.22(5)	3.1(8)	1.39(5)	14.8(6)	0.6(1)	6.34(8)	15(2)
0.3	8(2)	1.078	1.39(3)	14.6(3)	1.16(5)	2.3(8)	1.4(1)	15(1)	0.6(2)	5.3(2)	16(4)
0.4	7(2)	1.088	1.37(3)	14.8(3)	1.04(7)	0.6(9)	1.34(4)	15.1(5)	0.6(1)	4.67(4)	16(1)
0.5	7(2)	1.097					1.32(4)	15.2(5)	0.6(1)	4.20(2)	16(1)
0.6	6(2)	1.106					1.30(3)	15.3(4)	0.5(1)	3.86(1)	16.7(9)
0.7	6(2)	1.116					1.29(3)	15.3(4)	0.5(1)	3.59(1)	16.7(9)
0.8	6(2)	1.125					1.27(3)	15.3(4)	0.5(1)	3.36(1)	16.7(9)

[a] The cmc values (mM) obtained by surface tension measurements on H_2O solutions and the medium viscosity η (cp) used in the calculation are also reported. The esd's are indicated in parentheses. [b] cmc = 11(3)mM is obtained in D_2O solutions.

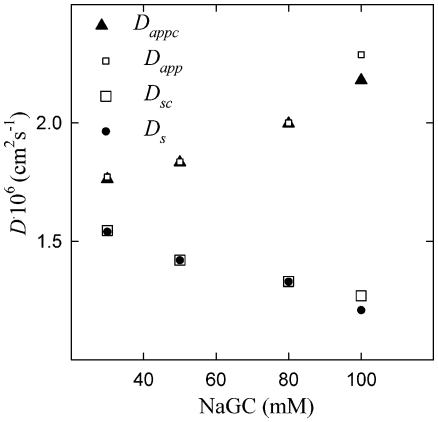

Figure 4. Experimental (D_{app} and D_s) and calculated (D_{appc} and D_{sc}) apparent and self-diffusion coefficients of NaGC D_2O solutions at 0.1 M NaCl as a function of NaGC concentration at 27 °C. D_{app} and D_s esd's are within 2%.

TABLE 2: Micellar Free-Diffusion Coefficient D_0 ($cm^2\ s^{-1}$), Hydrodynamic Radius a (Å), x_1 Values, Debye−Hückel Screening Length κ^{-1}(Å), and Aggregation Number n for NaGC D_2O Solutions at 0.1 M NaCl as a Function of NaGC Concentration (mM), Obtained on the Basis of the HC and DLVO Interaction Models[a]

	HC model			DLVO model			
NaGC	$D_o \times 10^6$	a	x_1	$D_o \times 10^6$	a	k^{-1}	n
30	1.59(3)	13.0(3)	1.4(1)	1.57(5)	13.2(6)	8.94(9)	11(2)
50	1.52(3)	13.6(3)	1.38(6)	1.47(5)	14.1(6)	8.70(9)	13(2)
80	1.50(3)	13.8(4)	1.36(4)	1.40(5)	14.7(6)	8.38(9)	15(2)
100	1.46(3)	14.2(3)	1.45(3)	1.35(5)	15.3(6)	8.18(9)	17(2)

[a] The esd's are reported in parentheses.

A comparison of the data presented in Tables 1 and 2 points out that similar hydrodynamic radii are observed by assuming the HC and the DLVO pair interaction potential. This conclusion is particularly interesting because it means that, despite its roughness, the HC model is suitable for inferring particle size information from diffusion measurements, and because of its simplicity, it can be easily used to interpret experimental data. An inspection of the a and n values shows that very slight micellar growth is induced by increasing both the NaCl and the surfactant concentration.

From the a and x_1 values, the thickness of the hard interaction shell $t = a(x_1 - 1)$ can be determined. The values so estimated are reported in Table 1. It is straightforward that the HC model can be applied to quantify the effect of particle interactions on the single D_{app} or D_s measurement if x_1 is known. Actually, because x_1 as a function of a and t can be expressed, this estimation can be performed if the t value is available. To provide an estimate of the t value, it should be related to an easily accessible physical variable defining the whole interaction potential. Unfortunately, the correlation between these data and the parameters characterizing the DLVO interaction potential is not easily understood. However, at the lowest NaCl concentrations (≤0.3 M) where the electrostatic repulsion strongly dominates the interaction potential, a rough relationship between t and the Debye−Hückel screening length can be checked. Because of the increasing effect of the attractive interactions, the $t\kappa$ products for these solutions slightly decrease by increasing the NaCl concentration. However, the decreasing trend is very smooth, and if this product is averaged over the range of 0.1−0.3 M NaCl, a value of 0.5(1) is obtained. Therefore, we conclude that $t \approx 0.5(1)\kappa^{-1}$ can be very crudely assumed in these conditions.

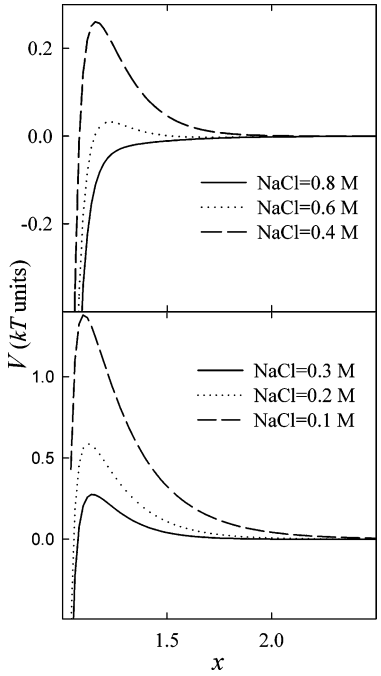

Figure 5. Plots of the DLVO pair interaction potential V as a function of the normalized distance x for different NaCl concentrations (T = 27 °C).

The pair interaction potentials derived with the fitting values obtained by assuming the DLVO interaction model are drawn in Figure 5. In agreement with the x_1 trend obtained from the HC model interpretation, an overall lowering of the interaction curve is observed by increasing the NaCl concentration because of the electrostatic repulsion screening. It is interesting that at the electrolyte molarity where the HC model begins to fail in the description of particle interaction, because of the dominance

of the attractive contribution, a small positive peak is still present in the DLVO potential.

V. Conclusions

We demonstrate that the experimental collective and self-diffusion coefficients of micelle solutions can be satisfactorily interpreted on the basis of the DLVO theory of colloid stability. A fit of both of the diffusion coefficients has been performed at different surfactant and/or added NaCl concentrations. The interpretation method allows us to consider both the effect of micellar growth and interaction potential variation. Hydrodynamic radii, aggregation numbers, and ionization degree of the micelle together with the intermicellar interaction potential in D_2O solutions can be estimated. At low NaCl concentration, where the electrostatic repulsion dominates the interaction potential, similar results are obtained if a model of a spherical particle with a rigid interaction shell of suitable thickness is used to interpret the experimental data.

Acknowledgment. This work was sponsored by the Italian Ministero dell'Istruzione, dell'Università e della Ricerca (Cofin no. 20020371541).

References and Notes

(1) Mazer, N. A.; Carey, M. C.; Kwasnick, R. F.; Benedek, G. B. *Biochemistry* **1979**, *18*, 3064.
(2) Schurtenberger, P.; Mazer, N.; Känzig, W. *J. Phys. Chem*. **1983**, *87*, 308.
(3) Janich, M.; Lange, J.; Graener, H.; Neubert, R. *J. Phys. Chem. B* **1998**, *102*, 5957.
(4) Briganti, G.; D'Archivio, A. A.; Galantini, L.; Giglio, E. *Langmuir* **1996**, *12*, 1180.
(5) D'Archivio, A. A.; Galantini, L.; Gavuzzo, E.; Giglio, E.; Scaramuzza, L. *Langmuir* **1996**, *12*, 4660.
(6) D'Alagni, M.; D'Archivio, A. A.; Galantini, L.; Giglio, E. *Langmuir* **1997**, *13*, 5811.
(7) Bonincontro, A.; Briganti, G.; D'Archivio, A. A.; Galantini, L.; Giglio, E. *J. Phys. Chem. B* **1997**, *101*, 10303.
(8) Bonincontro, A.; D'Archivio, A. A.; Galantini, L.; Giglio, E.; Punzo, F. *J. Phys. Chem. B* **1999**, *103*, 4986.
(9) Corti, M.; Degiorgio, V. *J. Phys. Chem.* **1981**, *85*, 711.
(10) Missel, P. J.; Mazer, N. A.; Benedek, G. B.; Young, C. Y.; Carey, M. C. *J. Phys. Chem.* **1980**, *84*, 1044.
(11) Porte, G.; Appel, J. *J. Phys. Chem*. **1982**, *85*, 2511.
(12) Young, C. Y.; Missel, P. J.; Mazer, N. A.; Benedek, G. B.; Carey, M. C. *J. Phys. Chem*. **1978**, *82*, 1375.
(13) D'Archivio, A. A.; Galantini, L.; Tettamanti, E. *J. Phys. Chem. B* **2000**, *104*, 9255.
(14) Galantini, L.; Pavel, N. V. *J. Chem. Phys.* **2003**, *118*, 2865.
(15) Dorshow, R.; Briggs, J.; Bunton, C. A.; Nicoli, D. F. *J. Phys. Chem.* **1982**, *86*, 2388.
(16) Dorshow, R. B.; Bunton, C. A.; Nicoli, D. F. *J. Phys. Chem*. **1983**, *87*, 1409.
(17) Ortega, F.; Bacaloglu, R.; McKanzie, D. C.; Bunton, C. A.; Nicoli, D. F. *J. Phys. Chem. B* **1990**, *94*, 501.
(18) Verwey, E. J. W.; Overbeck, J. Th. G. *Theory of the Stability of Lyophobic Colloids*; Elsevier: New York, 1948.
(19) Cichocki, B.; U. Felderhof, B. U. *J. Chem. Phys*. **1991**, *94*, 556.
(20) Siegert, A. J. F. *MIT Rad. Lab. Rep. No*. **1943**, 465.
(21) Koppel, D. E. *J. Chem. Phys*. **1972**, *57*, 4814.
(22) Stejskal, E. O.; Tanner, J. E. *J. Chem. Phys.* **1965**, *42*, 288.
(23) Karger, J.; Pfeifer, H.; Heink, W. *Adv. Magn. Reson.* **1987**, *12*, 1.
(24) Stilbs, P. *Prog. Nucl. Magn. Reson*. **1987**, *19*, 1.
(25) Price, W. S. *Concepts Magn. Reson*. **1997**, *9*, 299.
(26) Price, W. S. *Concepts Magn. Reson*. **1998**, *10*, 197.
(27) Tanner, J. E. *J. Chem. Phys*. **1970**, *52*, 2523.
(28) Wu, D.; Chen, A.; Johnson, C. S., Jr. *J. Magn. Reson., Ser. A* **1995**, *115*, 123.
(29) Pusey, P. N.; Tough, R. J. A. In *Dynamic Light Scattering*; Pecora, R., Ed.; Plenum: New York, 1985; Chapter 4.
(30) Cichocki, B.; Felderhof, B. U. *Phys. Rev. A* **1990**, *42*, 6024.
(31) Kato, T.; Seimiya, T. *J. Phys. Chem*. **1986**, *90*, 3159.
(32) Schurtenberger, P.; Lindman, B. *Biochemistry* **1985**, *24*, 7161.
(33) Batchelor, G. K. *J. Fluid Mech*. **1976**, *83*, 97.
(34) Felderhof, B. U. *J. Phys. A* **1978**, *11*, 929.
(35) Batchelor, G. K. *J. Fluid Mech*. **1983**, *131*, 155.
(36) Felderhof, B. U. *Physica A* **1977**, *89*, 373.
(37) Batchelor, G. K. *J. Fluid Mech*. **1976**, *74*, 1.
(38) Jeffrey, D. J.; Onishi, Y. *J. Fluid Mech* **1984**, *139*, 261.
(39) Venkatesan, M.; Hirtzel, C. S.; Rajagopalan, R. *J. Chem. Phys*. **1985**, *82*, 5685.
(40) Hamaker, H. C. *Physica (Amsterdam)* **1937**, *4*, 1058.
(41) Durchschlag, H.; Zipper, P. *J. Com. Esp. Deterg*. **1995**, *26*, 275.
(42) Galantini, L.; Giglio, E.; Leonelli, A.; Pavel, N. V. *J. Phys. Chem. B* **2004**, *108*, 3078.
(43) Sonntag, H.; Strenge, K. *Coagulation Kinetics and Structure Formation*; Deutscher der Wissenschaften: Berlin, 1987.